Optimal Low-Thrust Transfers to Synchronous Orbit

David C. Redding* and John V. Breakwell†
Stanford University, Stanford, California

The general problem of circle-to-circle transfer is examined for chemical rocket spacecraft, following Lawden's "primer vector" theory. Impulsive and near-impulsive transfers are analyzed to predict initial conditions for low-thrust transfers. A computer solution of the low-thrust problem is described. Results are presented for the low Earth orbit to geosynchronous orbit case, showing behavior of the optimal thrust direction, and developing transfer efficiency figures for a range of acceleration limits. Both fixed-thrust and fixed-acceleration propulsion systems are considered. The effect of multiple burns is discussed. Robbins's approximation for gravity loss is shown to be good for a large class of maneuvers.

Introduction

LOW-THRUST chemical spacecraft propulsion will enable the operation of large fragile space structures, by keeping small the forces they experience in transferring from low Earth parking orbit to their high operational orbits, usually geosynchronous. Other types of spacecraft also benefit from low-thrust propulsion, by using more efficient propulsion systems, by reducing the size of the transfer propulsion system, or by performing transfer maneuvers with station-keeping thrusters and eliminating a separate transfer propulsion system.

The minimum-fuel circle-to-circle transfer scheme in most practical cases is the Hohmann transfer, for which the two burns, at perigee and apogee, are considered to be impulses, changing the velocity instantaneously by Δv_0 and Δv_f, respectively. The impulses are directed parallel to the local horizontal, with a component in the direction of the plane change. The impulsive approximation is useful for estimating transfer fuel requirements in cases for which thrust-acceleration is high.

As successively lower limits are imposed on thrust-acceleration, the burn-arcs become longer. Since more of the acceleration is then applied farther from the optimum (perigee and apogee) points, these burns are necessarily less efficient, with the low thrust

$$\Delta v = \int_0^{t_b} A(t)\,\mathrm{d}t$$

being greater than the equivalent impulsive Δv. The difference $L = \Delta v - \Delta v_{\text{imp}}$ is termed gravity loss; it is a measure of transfer efficiency. The thrust direction during these burns is not parallel to the local horizontal, but is controlled to minimize fuel expenditure for given thrust or acceleration limits. A procedure for computing the optimal thrust direction history is given in this paper and illustrative results are given.

Two-burn transfer at very low thrust levels will have long burn-arcs and incur large gravity losses. However, if a different approach is adopted, the loss can be kept arbitrarily low even for the lowest thrust levels. By applying only part of the perigee Δv initially, then coasting around the partially raised orbit to near perigee again and repeating, the burn-arc lengths are shortened and the total gravity loss is reduced by roughly $1/N^2$, where N is the number of perigee burns; likewise at apogee. It is clear that although this procedure yields a savings in gravity loss, there is also a considerable penalty in trip time: total time increases roughly as N. The analysis presented here is valid for both the high-loss case and the multiple-burn case. A detailed study of results for the optimal multiple-burn case for a large range of trip times and thrust limits is presented in Ref. 1.

We consider two types of propulsion system in this paper. Type 1 is fixed-acceleration, presumably a chemical rocket continuously throttled to maintain acceleration at some allowed maximum. Type 2 is fixed-thrust, which has its lowest acceleration initially and reaches its maximum acceleration only at the end of the final burn, when mass is the least. Fixed-thrust transfers are therefore less efficient than fixed-acceleration transfers, other things being equal, if an acceleration limit is imposed.

Analytical Approach

Previous studies of low-thrust transfer problems have been mainly of two types. Studies have been done using simple nonoptimal control laws, such as horizontal or tangential pointing, and "patching" methods of constructing transfer trajectories.[2] This approach has been used to solve small and large transfers, short and long burn-arc transfers, one burn and many burn transfers, often in unpublished studies.

The other main approach is by the "averaged elements" formulation of the optimal control problem, as used by Edelbaum and others.[3] In this approach, the state vector is composed of orbital elements, not necessarily including position of the spacecraft, and change per orbit of the elements is assumed to be small. This allows the Hamiltonian to be averaged, enormously reducing computational effort: Some cases are solvable in closed form; others are integrable in time-steps of a day or more. Small perturbation forces such as those due to oblateness are easily included as averaged changes to the state.

The main disadvantage of the averaging approach is that the thrust is required to be too low to be of general interest. The accelerations permitted are typical of electrical propulsion, not chemical rockets.

Our approach is by the "primer vector" theory developed by Lawden in the 1950's (Ref. 4). Here the state vector is composed of the position and velocity vectors and the spacecraft mass. Lawden's solution of the optimal control problem provides a switching function for the thrust as well as a variable thrust direction, as detailed below. This formulation is related to the orbital-elements formulation by a canonical transformation. The difference between the two

Presented as Paper 81-130 at the AAS/AIAA Astrodynamics Specialist Conference, Lake Tahoe, Nev., Aug. 3-5, 1981; submitted May 7, 1982; revision received May 7, 1983.

*Graduate Student, Department of Aeronautics and Astronautics. Currently Staff Engineer, Charles Stark Draper Laboratory, Cambridge, Mass. Student Member AIAA.

†Professor, Department of Aeronautics and Astronautics. Fellow AIAA.

approaches is mainly that we do not use averaging. Our solutions are therefore exact within the definition of our problem (we have not yet considered oblateness or other perturbations). They are also optimal and provide detailed information on the optimal thrust direction.

Another difference is in the cost function. Most studies using averaged elements are for power-limited spacecraft and minimize $\int A^2 \mathrm{d}t$. It is more appropriate for chemical propulsion systems to minimize the added velocity

$$\Delta v = \int_{t_0}^{t_b} A(t)\,\mathrm{d}t,$$

which is equivalent to maximizing the final mass.

Problems associated with our approach are that solution can be difficult due to extreme sensitivity of the trajectory to the initial adjoints, and that computation can be costly for long duration transfers. The first problem is reduced by developing good analytical estimates of the initial adjoints and by slaving one of the most sensitive parameters to another, less sensitive parameter, thereby insuring that the terminal state is fairly linear in the chosen parameters. The second problem is partially dealt with by analytical, as opposed to numerical, treatment of the coasting arcs.

Analysis

The following discussion is primarily in terms of fixed-acceleration (type 1) transfers; except where noted it can be considered to hold for fixed-thrust transfers as well.

The spacecraft equations of motion are

$$\dot{r} = v \tag{1}$$

$$\dot{v} = -(\mu r/r^3) + A\hat{p} \tag{2}$$

Here $\hat{p}$ denotes the thrust direction. For type 2 transfers,

$$\dot{r} = v \tag{3}$$

$$\dot{v} = -(\mu r/r^3) + (T/m)\hat{p} \tag{4}$$

$$(\dot{m}/m_0) = -(T/m_0 c) \qquad c = I_{sp} g_0 \tag{5}$$

We wish to minimize the imparted velocity by maximizing its negative:

$$J = -\int_{t_0}^{t_f} A(t)\,\mathrm{d}t = \Delta v \tag{6}$$

The Hamiltonian (to be maximized) is then

$$H = -kA + \lambda_r \cdot v + \lambda_v \cdot [-(\mu r/r^3) + A\hat{p}] \tag{7}$$

For type 2 transfers,

$$H = -\lambda_m (kT/c) + \lambda_r \cdot v + \lambda_v \cdot [-(\mu r/r^3) + (T/m)\hat{p}] \tag{8}$$

Adjoint equations are [here, $\Gamma(r)$ is the gravity-gradient tensor]

$$\dot{\lambda}_r = -\Gamma(r) \cdot \lambda_v \tag{9}$$

$$\dot{\lambda}_v = -\lambda_r \tag{10}$$

$$\dot{\lambda}_m = T|\lambda_v|/m^2 \tag{11}$$

Note that the equations for λ_v and λ_r can be written:

$$\ddot{\lambda}_v = -\dot{\lambda}_r = \Gamma(r)\lambda_v \tag{12}$$

This is in the form of the familiar perturbed-orbit problem and can be solved for λ_v analytically over coasting arcs using the results of Danby.[5]

Lawden showed that the magnitude of the acceleration A is given by a switch function S:

$$S = |\lambda_v| - |\lambda_{v_0}| \tag{13}$$

$$A = A_M \text{ (the maximum allowed) when } S > 0$$

$$= 0 \qquad \text{when } S < 0 \tag{14}$$

For fixed-thrust transfers,

$$S = |\lambda_v| - m\lambda_m/c \tag{15}$$

$$T = T_M \text{ when } S > 0$$

$$= 0 \quad \text{when } S < 0 \tag{16}$$

Since we are solving a time-free problem, $H = 0$; and λ_m remains constant during coasting arcs. Alternative switching functions can be used that make it unnecessary to integrate Eq. (11). These are

$$S_{\text{off}} = H - \text{thrust terms} = \lambda_r \cdot v + \lambda_v \cdot (-\mu r/r^3) \tag{17}$$

$$S_{\text{on}} = |\lambda_v| - |\lambda_{v_{\text{prev}}}| \tag{18}$$

Thrust is turned off when S_{off} reaches zero from below; the next burn starts when $|\lambda_v|$ reaches its value at the end of the previous burn. Note that the thrust/mass dynamics do not enter into these expressions, so that these switch functions are valid for any autonomous thrust-mass dynamics, such as for blowdown propulsion.

The optimal thrust direction $\hat{p}$ is given by Lawden's primer vector, λ_v in our notation:

$$\hat{p} = \lambda_v / |\lambda_v| \tag{19}$$

Thus we burn in the direction $\hat{p}$ while $S > 0$ and coast while $S < 0$, as illustrated in Fig. 1.

The system equations (1-5) and (9-11), if integrated forward in the proper fashion from some initial values of the state and adjoint until the final switchoff, always give a locally optimal trajectory between that initial state and the resulting final state. Now the trick is to find the particular initial conditions that give the specific optimal trajectory that has the desired final state. In the next section we do this for the impulsive case.

Impulsive Transfers

For the purpose of illustration and to obtain some useful formulas, we will now examine the familiar two-impulse transfer (Hohmann with plane change) using the primer vector theory. Here the acceleration A is infinite and so of zero duration; S now comes up and just touches the switch line at the burn points, as shown in Fig. 2. Since S is tangent

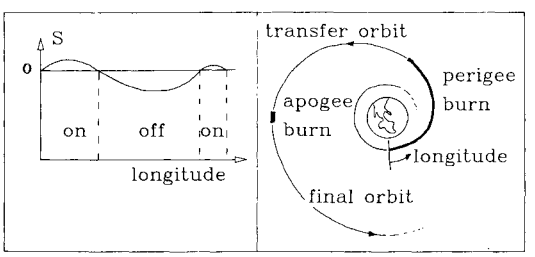

Fig. 1 Behavior of the switch function S.

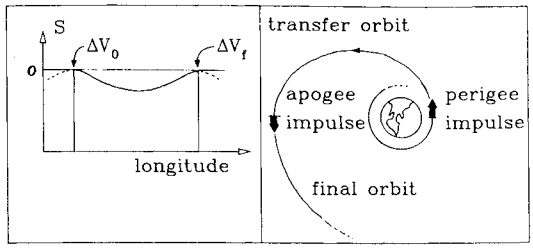

Fig. 2 *S* **in the impulsive case.**

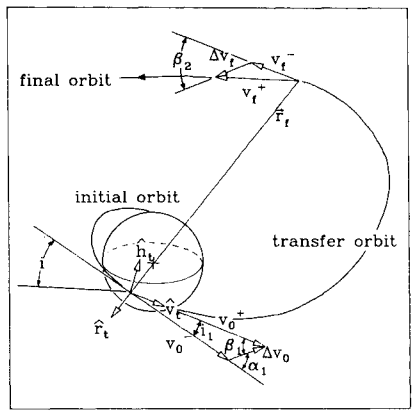

Fig. 3 Impulsive transfer geometry.

to the $S=0$ line at these points, its instantaneous rate of change is zero and we can write

$$\frac{\mathrm{d}}{\mathrm{d}t}S=\frac{\mathrm{d}}{\mathrm{d}t}\,|\lambda_v\cdot\lambda_v|^{1/2}=-\frac{\lambda_v\cdot\lambda_r}{|\lambda_v|}=0 \tag{20}$$

Hence $\lambda_v\cdot\lambda_r=0$ and there is no component of λ_r in the direction of λ_v at the burn points.

The optimal direction of the perigee impulse is known to be forward in the direction of the initial circular velocity and upward in the direction of the plane change, with no radial component. Using the $(\hat{r}_t,\ \hat{v}_t,\ \hat{h}_t)$ coordinate system, which refers to conditions at the transfer orbit perigee, we normalize the primer vector to its initial value and express its direction in terms of an out-of-plane pointing angle β_1, as shown in Fig. 3:

$$\lambda_{v_0}=\cos\beta_1\hat{v}_t+\sin\beta_1\hat{h}_t \tag{21}$$

Applying the conditions $\lambda_{v_0}\cdot\lambda_{r_0}=0$ and $H=0$, we find that λ_{r_0} is parallel to $\hat{r}_t$. This is expresed in terms of a parameter ν:

$$\lambda_{r_0}=\nu\hat{r}_t \tag{22}$$

The problem is now to find the β_1 and ν that give the desired circle-to-circle transfer with plane change i.

Recalling that the form of the adjoint equation is that of the perturbed orbit problem, we use formulas from Danby[5] to find the adjoints at the apogee burn:

$$\begin{bmatrix}\lambda_{v_f}\\ -\lambda_{r_f}\end{bmatrix}=\Phi(t_f,0)\begin{bmatrix}\lambda_{v_0}\\ -\lambda_{r_0}\end{bmatrix} \tag{23}$$

In particular,

$$\lambda_{v_f}=\left(\frac{3-e}{1-e}\cos\beta_1-\frac{4\nu}{n}\sqrt{\frac{1-e}{1+e}}\right)\hat{v}_t-\frac{1+e}{1-e}\sin\beta_1\hat{h}_t \tag{24}$$

$$\lambda_{r_f}=\left(\frac{(3+e)(1-e)}{(1+e)^2}\nu-\frac{2n\cos\beta_1}{(1+e)\sqrt{1-e^2}}\right)\hat{r}_t\equiv-\nu_f\hat{r}_t \tag{25}$$

Here, $n=\sqrt{\mu/a^3}$ and e refer to the transfer orbit and are determined from r_0 and r_f by Keplerian formulas.

The optimal apogee impulse, like the optimal perigee impulse, has components forward and in the direction of the plane change (down). That is, $\lambda_{v_f}\cdot\hat{v}_t<0$. Recalling that $|\lambda_{v_f}|=|\lambda_{v_0}|$, as both are burn points, we now solve for ν, finding that

$$\nu=\frac{n}{4}\sqrt{\frac{1+e}{1-e}}\left[\frac{3-e}{1-e}\cos\beta_1+\sqrt{1-\left(\frac{1+e}{1-e}\sin\beta_1\right)^2}\right] \tag{26}$$

An alternative expression for λ_{v_f} is in terms of the pointing angle β_2:

$$\lambda_{v_f}=-\cos\beta_2\hat{v}_t+\sin\beta_2\hat{h}_t \tag{27}$$

Comparing Eqs. (24), (26), and (27), we see that for optimality,

$$\sin\beta_2=\frac{1+e}{1-e}\sin\beta_1 \tag{28}$$

Keplerian formulas and the transfer geometry given on Fig. 3 yield

$$\frac{\sin(\beta_1+i_1)}{\sin\beta_1}=\frac{v_0^+}{v_0^-}=\sqrt{1+e} \tag{29}$$

$$\frac{\sin(\beta_2-i_2)}{\sin\beta_2}=\frac{v_f^-}{v_f^+}=\sqrt{1-e} \tag{30}$$

$$i_1+i_2=\text{desired } i \tag{31}$$

Equations (28-31) are solved iteratively for β_1; Δv_0 and Δv_f are computed from the pointing angles and r_0 and r_f in the usual way.

Having now found ν and β_1, and thus the initial adjoints λ_{r_0} and λ_{v_0}, our problem is solved. To transfer from r_0 to r_f with plane change i, we apply an initial impulse Δv_0 along λ_{v_0} and coast along the resulting transfer orbit while keeping track of λ_v and λ_r. $|\lambda_v|$ will return to its initial value at apogee, at which point we apply Δv_f along λ_{v_f} to complete the transfer.

A word about ν. Recalling that $\lambda_r=-\dot{\lambda}_v$ and $\lambda_{r_0}\cdot\lambda_{v_0}=\lambda_{r_f}\cdot\lambda_{v_f}=0$, ν is seen to be the optimal turn rate of the thrust direction at the perigee impulse point. Likewise, from Eq. (25), the optimal thrust direction turn rate at apogee is

$$\nu_f=\frac{(3+e)(1-e)}{(1+e)^2}\nu-\frac{2n\cos\beta_1}{(1+e)\sqrt{1-e^2}} \tag{32}$$

High-Acceleration Transfers

If the transfer acceleration is large but finite, so that the burns are of short duration, the transfer will closely resemble the impulsive case, and certain approximations can be made to obtain formulas for the initial position and adjoints. These formulas provide usable initial conditions for the system equations, which can then be solved numerically using the computer program described below. It turns out that the initial guesses provided by these formulas are good even for fairly low acceleration. Gravity loss for high-acceleration transfers can be estimated using a formula derived by Robbins.[6]

We now compare a fixed, high-acceleration perigee burn with an impulsive maneuver of equivalent effect. We assume that the turn rate ν is constant throughout the burn, which is true to order $(1/A)$. It is then easy to show that the equivalent

impulse occurs at a time $t_B/2$ after initiation of the high-A burn and is in the direction of λ_v at that time. Here, t_B is the burn time, approximated as $t_B = \Delta v/A$.

As the proper location of the impulse is at the node of the initial and transfer orbits, the initial position $\Delta\theta_0$ of the spacecraft relative to the node is written (see Fig. 4):

$$\Delta\theta_0 = \tfrac{1}{2} n_0 t_B = \frac{n_0 \Delta v_0}{2A} \tag{33}$$

Here n_0 is the mean motion of the initial circular orbit. The initial state of the spacecraft is completely specified by Eq. (33), the initial inclination and radius, and the fact that the initial orbit is circular.

The initial adjoints in the high-A case are close to those of the impulsive case. λ_{v_0} has major components forward and in the direction of plane change as before, but now also has a small radial component, denoted by $-\epsilon$. Using coordinates $(\hat{r}_0, \hat{v}_0, \hat{h}_0)$ which refer to the initial orbit, we write

$$\lambda_{v_0} = -\epsilon \hat{r}_0 + \cos\alpha_I \hat{v}_0 + \sin\alpha_I \hat{h}_0 \tag{34}$$

Here α_I is a pointing angle with respect to the initial orbital plane, which to $O(1/A^2)$ is the same as for the impulsive case (see Figs. 3 and 4):

$$\alpha_I = (\beta_I + i_I)_{\text{imp}} \tag{35}$$

The major component of λ_{r_0}, as for the impulsive case, is in the radial direction. These radial components are nearly equal:

$$\lambda_r \cdot \hat{r}_0 = \nu + O(1/A) \tag{36}$$

We find the forward component of λ_{r_0} by applying the $H = 0$ condition:

$$\lambda_{r_0} \cdot v = \lambda_{v_0} \cdot (\mu r/r^3) \tag{37}$$

$$\lambda_{r_0} \cdot v_0 = (\mu/r_0^3)(\epsilon/v_0) = -\epsilon n_0 \tag{38}$$

$$(\text{as } v_0 = \sqrt{\mu/r_0} \quad \text{and} \quad n_0 = \sqrt{\mu/r_0^3})$$

The condition $\lambda_{r_0} \cdot \lambda_{v_0} = 0$ does not obtain in this case, and λ_{r_0} has a small component along $\hat{h}_0$, denoted by ρn_0, say. We now write

$$\lambda_{r_0} = [\nu + O(1/A)]\hat{r}_0 - \epsilon n_0 \hat{v}_0 + \rho n_0 \hat{h}_0 \tag{39}$$

To find an expression for ϵ, we compare the equivalent-impulse primer vector with the high-A primer vector at the half-burn time. We can write the equivalent-impulse primer in terms of coordinates $(\hat{r}_I, \hat{v}_I, \hat{h}_I)$ which refer to conditions at the node:

$$\lambda_{v_{\text{imp}}} = \cos\alpha_I \hat{v}_I + \sin\alpha_I \hat{h}_I \tag{40}$$

At the impulse time $t_B/2$, the spacecraft is at the node, angular distance $\Delta\theta_0$ from its initial position, so that (as $\Delta\theta_0$ is small)

$$\hat{v}_I = \hat{v}_0 - \Delta\theta_0 \hat{r}_0 \quad \text{and} \quad \hat{h}_I = \hat{h}_0 \tag{41}$$

$$\lambda_{v_{\text{imp}}} = -\Delta\theta_0 \cos\alpha_I \hat{r}_0 + \cos\alpha_I \hat{v}_0 + \sin\alpha_I \hat{h}_0 \tag{42}$$

At this time the high-A primer vector is the same as $\lambda_{v_{\text{imp}}}$, having rotated inward at a rate ν from its initial orientation:

$$\lambda_v = [-\epsilon - \nu(t_B/2)]\hat{r}_0 + \cos\alpha_I \hat{v}_0 + \sin\alpha_I \hat{h}_0 \tag{43}$$

Equating expressions (42) and (43), we find

$$\epsilon = \Delta\theta_0 \cos\alpha_I - \nu\frac{t_B}{2} = \frac{\Delta v_0}{2A}(n_0 \cos\alpha_I - \nu) \tag{44}$$

The final parameter ρ is determined by the requirement that $|\lambda_v|$ return to its initial value (from higher values) at time t_B, as illustrated on Fig. 1. Here,

$$\frac{\mathrm{d}}{\mathrm{d}t}(|\lambda_v^2|) = -2\lambda_v \cdot \lambda_r = -2\lambda_{v_0} \cdot \lambda_{r_0} + O\left(\frac{1}{A^2}\right) \tag{45}$$

$$\frac{\mathrm{d}}{\mathrm{d}t}(|\lambda_v^2|) = 2[\epsilon(\nu + n_0 \cos\alpha_I) + \rho n_0 \sin\alpha_I] + O\left(\frac{1}{A^2}\right) \tag{46}$$

The second derivative of $|\lambda_v^2|$ is the same as for the impulsive case, to $O(1/A)$:

$$\frac{\mathrm{d}^2}{\mathrm{d}t^2}(|\lambda_v|^2) = 2|\lambda_r|^2 + 2\lambda_v \cdot \frac{\mu}{r^3}[3(\lambda_v \cdot \hat{r})\hat{r} - \lambda_v] \tag{47}$$

$$\frac{\mathrm{d}^2}{\mathrm{d}t^2}(|\lambda_v|^2) = 2(\nu^2 - n_0^2) \tag{48}$$

Expanding about $t = 0$ to obtain $|\lambda_v^2|$ [for t of order $(1/A)$],

$$|\lambda_v(t)|^2 = |\lambda_v(0)|^2 + 2t[\epsilon(\nu + n_0 \cos\alpha_I) + \rho n_0 \sin\alpha_I] - (n_0^2 - \nu^2)t^2 + 0(1/A^3) \tag{49}$$

At time t_B, $|\lambda_v^2| = |\lambda_{v_0}^2|$, and so,

$$(n_0^2 - \nu^2)t_B = 2\epsilon(\nu + n_0 \cos\alpha_I) + 2\rho n_0 \sin\alpha_I \tag{50}$$

Substituting for ϵ and t_B, we finally obtain

$$\rho = \frac{n_0 \Delta v_0}{2A} \sin\alpha_I \tag{51}$$

Thus the initial adjoints and position for high-A transfer are found approximately from the equivalent impulsive transfer and formulas (26), (33-35), (39), (44), and (51). A complete transfer is obtained by integrating the state and adjoint equations forward from these initial conditions, burning as indicated by the primer vector, until the final orbit is achieved.

The case of a single, high constant-thrust perigee burn is similar to the high-A case. Here, the position and velocity at burnout time t_B are the same (to order $1/A_0$) as for an equivalent-impulse at time t_c in the direction of $\lambda_v(t_c)$, where

$$\int_0^{t_B} (t - t_c) A(t)\,\mathrm{d}t = 0 \tag{52}$$

Here,

$$A(t) = T_M/m \quad \text{and} \quad \dot{m} = -(T_M/C) \tag{53}$$

Centroid time t_c is thus

$$t_c = \frac{c}{T_M}\left(m_0 - \frac{m_0 - m_I}{\ln(m_0/m_I)}\right) \tag{54}$$

Note that if $A(t) = A$ is constant, $t_c = t_B/2$.

The initial adjoints have the same form as in Eqs. (34) and (39). Repeating the high-A arguments, we find $\Delta\theta_0$ and ϵ for high-T to be

$$\Delta\theta_0 = n_0 t_c \tag{55}$$

$$\epsilon = (n_0 \cos\alpha_I - \nu)t_c \tag{56}$$

The parameter ρ is determined from conditions at the end of the burn as before. For $S = |\lambda_v| - m\lambda_m/c$,

$$\dot{S} = \frac{\mathrm{d}}{\mathrm{d}t}|\lambda_v| + \frac{T_M \lambda_m}{c^2} - \frac{m}{c}\frac{T_M}{m^2}|\lambda_v| \tag{57}$$

$$\dot{S} = -\frac{A(t)}{c}S + \frac{\mathrm{d}}{\mathrm{d}t}|\lambda_v| \tag{58}$$

At the end of the burn, $t = t_B$ and $S = 0$, so that

$$\int_0^{t_B} \exp\left[\int_0^t \frac{A(t)}{c}\,\mathrm{d}t\frac{\mathrm{d}}{\mathrm{d}t}\right]\frac{\mathrm{d}}{\mathrm{d}t}|\lambda_v|\,\mathrm{d}t = 0 \tag{59}$$

Here,

$$\frac{\mathrm{d}}{\mathrm{d}t}|\lambda_v| = \frac{1}{2}\frac{\mathrm{d}}{\mathrm{d}t}(|\lambda_v|^2) + 0\left(\frac{1}{A^2}\right)$$

$$= \epsilon(n_0\cos\alpha_1 + \nu) + \rho n_0 \sin\alpha_1 - (n_0^2 - \nu^2)t + 0\left(\frac{1}{A^2}\right) \tag{60}$$

$$\exp\left[\int_0^t \frac{A(t)}{c}\,\mathrm{d}t\right] = \frac{m_0}{m(t)} = \frac{m_0}{T_M}A(t) \tag{61}$$

The condition that S return to zero at time t_B may thus be written

$$\int_0^{t_B} A(t)\,[\epsilon(n_0\cos\alpha_1 + \nu) + n_0\sin\alpha_1 - (n_0^2 - \nu^2)t]\,\mathrm{d}t = 0 \tag{62}$$

Applying condition (52), we find

$$\epsilon(n_0\cos\alpha_1 + \nu) + \rho n_0\sin\alpha_1 - (n_0^2 - \nu^2)t_c = 0 \tag{63}$$

Substituting for ϵ and simplifying, we finally obtain

$$\rho = n_0 t_c \sin\alpha_1 \tag{64}$$

Approximate initial position and adjoints for high-T transfer can now be computed from the equivalent impulsive transfer and formulas (26), (34), (35), (39), (54-56), and (64).

To complete our comparison of high-acceleration perigee burns with their equivalent impulsive maneuvers, we can estimate the gravity loss L, and thus the finite-thrust Δv, by applying Robbins's formula[1,6]

$$\text{Loss} = (\Delta v - \Delta v_{\text{imp}}) = \tfrac{1}{2}(\mu/r^3 - \omega_{\text{opt}}^2)\int (t - t_c)^2 A(t)\,\mathrm{d}t \tag{65}$$

Here ω_{opt} is the optimal thrust-vector turn rate at the equivalent impulse (ν in our notation). For a fixed-A perigee burn,

$$L = \frac{(\Delta v_{\text{imp}})^2}{24A^2}(n_0^2 - \nu^2) \tag{66}$$

For fixed-thrust,

$$L = \frac{1}{(T/m_0)^2}\left[(n_0^2 - \omega_{\text{opt}}^2)\frac{c^3}{2}\left(1 - \frac{m}{m_0}\right)^2\left(\frac{1}{1 - m/m_0} - \frac{1}{2} + \frac{1}{\ell_n(m/m_0)}\right)\right] \tag{67}$$

As mentioned in the introduction, it is sometimes useful to subdivide the perigee burn and/or apogee burn of a transfer, to reduce the average burn-arc length and so reduce gravity loss. It is straightforward to show (for high constant acceleration) that the intermediate burns should be of equal magnitude. For N perigee burns, then, each burn should have

$$\Delta v_i = \frac{(\Delta v_0)_{\text{imp}}}{N} \tag{68}$$

The formulas for the initial adjoint parameters in the fixed-A multiple perigee burn case are obained by replacing Δv_0 wherever it appears by $\Delta v_0/N$:

$$\epsilon = \frac{\Delta v_0}{2NA}(n_0\cos\alpha_1 - \nu) \tag{69}$$

$$\rho = \frac{n_0 \Delta v_0}{2NA}\sin\alpha_1 \tag{70}$$

$$\Delta\theta_0 = \frac{n_0 \Delta v_0}{2NA} \tag{71}$$

The complete transfer gravity loss is (for N perigee and M apogee burns)

$$L = \frac{\Delta v_0^3}{24(NA)^2}(n_0^2 - \nu^2) + \frac{\Delta v_f^3}{24(MA)^2}(n_f^2 - \nu_f^2) \tag{72}$$

The case of fixed-T multiple perigee burn transfer is more complex, as here the burns are not quite equal. A procedure for finding the optimal intermediate mass ratios m_i/m_{i-1} is given in Ref. 1. This procedure can be applied to find the mass ratio for the first perigee burn; using this in Eq. (54) gives an accurate value of t_c for determining $\Delta\theta_0$, ϵ, and ρ. However, it is usually adequate to make the approximation

$$t_c = \frac{cm_0}{NT}\left(1 + \frac{1 - m/m_0}{\ell_n(m/m_0)}\right) \tag{73}$$

Here m/m_0 refers to the one-burn maneuver.

It is very significant that A and T/m_0 appear in the initial parameter formulas only as products with N. This means that any transfer for which $NA_0 = C$ will have essentially the same initial adjoints and position as any similar transfer for which $NA_0 = C$. These transfers will also all incur about the same gravity loss at perigee, as shown for the fixed-A by formula (72). This greatly facilitates extending results from single to multiple burn cases.

Computation of Low-Acceleration Transfers

In the previous section, we obtained expressions for the initial adjoint and position vectors of the spacecraft in cases where thrust-acceleration is high. In this section, we describe the computer program that solves the complete transfer problem for high- and low-acceleration cases, starting from thee initial conditions.

If the initial position and adjoints are known exactly, solution is assured: The system equations (1-5) and (9-11) are simply integrated forward, following Eqs. (13-16), until the final burn is completed. This will give a complete optimal transfer time-history and trip-time and gravity loss figures.

The formulas of the previous section are not exact, however. It is necessary to improve the initial guesses they provide to obtain the desired final state. This improvement is done iteratively using the "shooting method" of computation.

Here the initial state and adjoint determined by the guessed initial parameters are run forward until the final burn is completed; this provides a nominal trajectory with final conditions near the desired final conditions. The initial parameters are then each perturbed in turn, with corresponding final states obtained by integrating each perturbed trajectory. The sensitivity matrix of the final conditions to the initial parameters is then used in a linear interpolation scheme to obtain improved initial parameters.

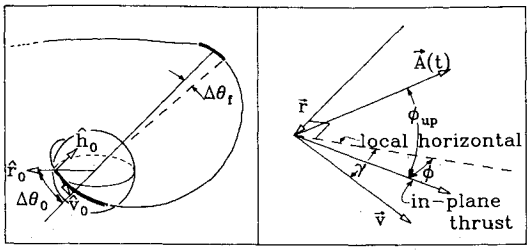

Fig. 4 Finite-thrust transfer geometry.

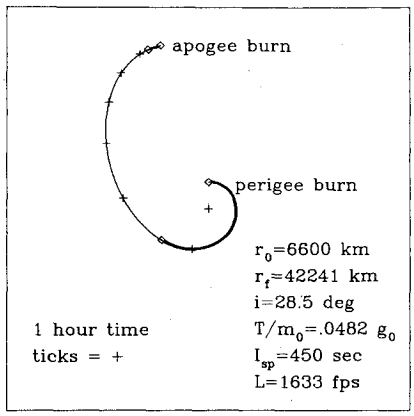

Fig. 5 Trajectory for example 1 (projected onto the transfer plane).

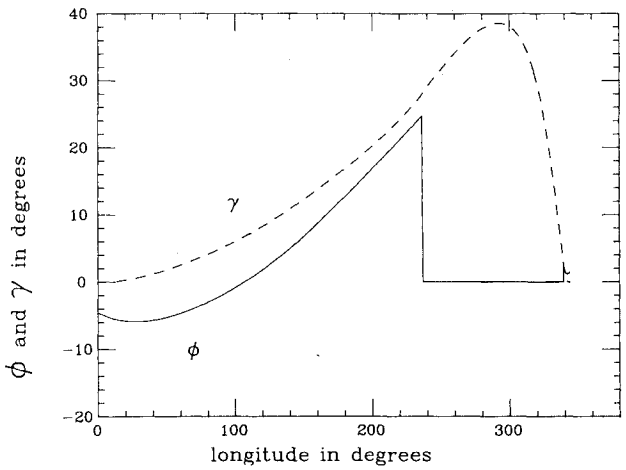

Fig. 6 In-plane pointing angle vs longitude for example 1.

The process is repeated using these initial guesses until the final conditons are exactly matched.

The success of this method depends on the final conditions being fairly linear in the initial parameters. We have some freedom in choosing particular final conditions and initial parameters to use in computation; it is best to choose initial parameters that affect particular elements of the final state in linear fashion. For example, the duration of the perigee burn directly affects the apogee radius, and the duration of the perigee burn depends mainly on the parameter ϵ, so that the final r is nearly linear in ϵ. Thus ϵ is a good initial parameter, and r is a good final conditon to be matched.

Not all the initial adjoint parameters of the previous section are good initial parameters for the program. The apogee burn duration, which determines the final velocity v_f, is a highly nonlinear function of the height of the apogee maximum of the switch function S (see Fig. 1). This height is, in turn, an essentially linear function of the parameter ν. Hence v_f is a highly nonlinear function of ν, and ν is a poor choice for an initial parameter to determine v_f.

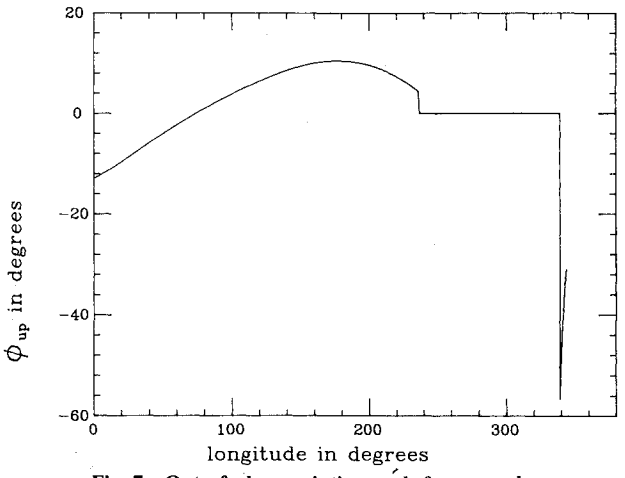

Fig. 7 Out-of-plane pointing angle for example.

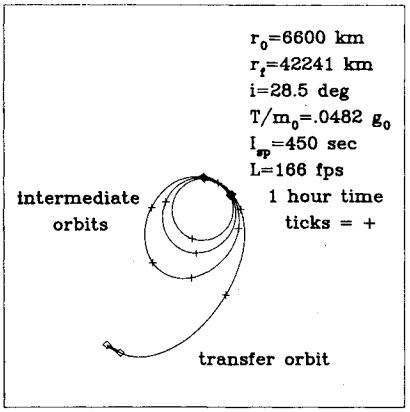

Fig. 8 Trajectory for example 2 (projected onto the transfer plane).

A better choice is the parameter $\Delta\theta_f$, the angular distance of the apogee burn turn-on point from the transfer orbit apogee (see Fig. 4). For high accelerations $\Delta\theta_f$ can be approximated:

$$\Delta\theta_f = \left(\frac{\Delta v_f}{2MA}\right)\left(\frac{v_f^-}{r_f}\right) \qquad \text{for type 1} \qquad (74)$$

$$\Delta\theta_f = \left(\frac{t_c}{M}\right)\left(\frac{v_f^-}{r_f}\right) \qquad \text{for type 2} \qquad (75)$$

Here M is the number of perigee burns. By determining the apogee burn turn-on point, $\Delta\theta_f$ directly controls the duration of the apogee burns; hence v_f is nearly linear in $\Delta\theta_f$.

We incorporate $\Delta\theta_f$ into the determination of the initial adjoints in an "inner loop" to the computation of each trajectory: holding the initial parameters constant, ν is adjusted iteratively until apogee turn-on occurs precisely at the true anomaly $(2N-1)\pi+\Delta\theta_f$. The complete trajectory is then computed using this value of ν.

The chosen set of initial parameters is ϵ, $\Delta\theta_f$, ρ, α_1, and $\Delta\theta_0$. The final conditions to be matched are r_f, v_f, z_f, $\dot{z}_f$, and γ, where z is height above the desired final plane and γ is the flight-path angle.

As acceleration levels are lowered, there comes a point when the formulas for the initial parameters no longer give adequate guesses. For LEO-GEO transfer this occurs when $NA_0 < \frac{1}{4}g_0$; for transfer from 6600 to 7800 km, it occurs when $NA_0 < (1/60)g_0$. For initial accelerations lower than this, initial parameters can be guessed by gradually extrapolating on results for higher accelerations.

It was pointed out in the previous section that if the number of perigee burns and initial acceleration for a specific transfer

are changed so that the product NA_0 is constant, the resulting transfer will have nearly the same initial parameters and gravity loss. This allows quick and reliable extension of particular $N=1$ results to large N cases.

Results

In this section, we present results for transfer from a low Earth orbit (6600 km, 28.5-deg inclination) to geosynchronous orbit (42,241 km, 0-deg inclination). We present two specific example transfers, showing detail of their time histories. We then give initial parameters and gravity loss results for a range of initial accelerations and numbers of burns.

Both examples are constant-thrust transfers with specific impulse $I_{sp}=450$ s and initial acceleration $T/m_0=0.0482$ $g_0=1.552$ ft/s^2. The difference between them is in the numbers of perigee burns. Example 1 uses one long perigee burn and one apogee burn; a large gravity loss is incurred at perigee. Example 2 uses four perigee burns to reduce gravity loss.

The thrust direction is specified by an in-plane pointing angle ϕ and an out-of-plane pointing angle ϕ_{up}, as shown on Fig. 4.

The instantaneous-plane trajectory of the single-burn example is shown on Fig. 5. The perigee burn takes 1.32 hours and 236 deg of longitude. Mass change due to propellant expenditure is 66%, so that acceleration rises from 0.0482 to 0.1417 g_0. Eccentricity and inclination of the transfer orbit are 0.6234 and 25.9 deg, respectively, as opposed to 0.730 and 26.3 for the impulsive case. Total trip time is 6.76 h; gravity loss is 1633 ft/s.

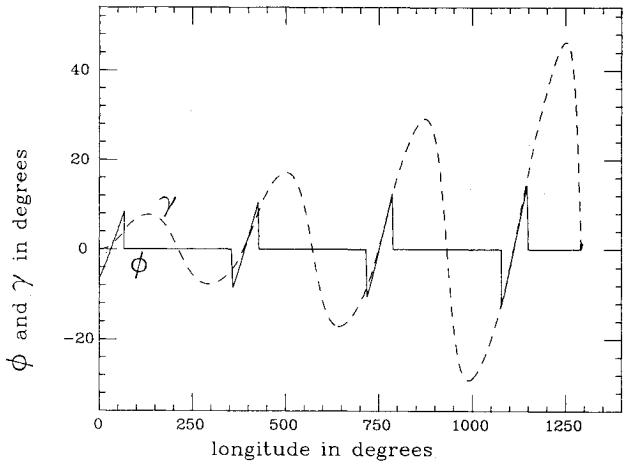

Fig. 9 In-plane pointing angle vs longitude for example 2.

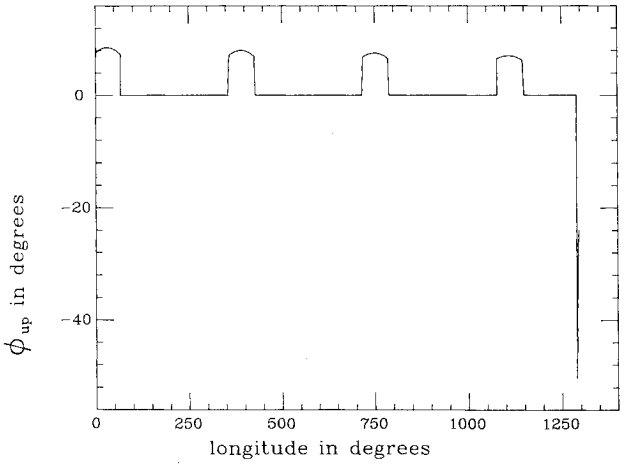

Fig. 10 Out-of-plane pointing angle for example 2.

The behavior of the thrust direction is shown in Figs. 6 and 7. The in-plane component of the thrust vector initially points inward of the local horizontal but rotates to point outward by 25 deg at the end of the perigee burn. Throughout the perigee burn, the thrust points inward of the velocity vector. During the apogee burn, the thrust points slightly outward.

The out-of-plane thrust component is directed downward until the spacecraft is about 90 deg from the node of the initial and final orbits; it is directed upward from then until termination of the perigee burn, with a maximum at the node. The resulting torque on the orbit causes precession about the line of nodes. The major part of the plane change is at apogee, where lower speeds mean a greater change in direction is possible for a given Δv.

The turn rate of the optimal thrust direction rises from 0.00126 rad/s initially to a maximum of 0.00148 rad/s at about the time the out-of-plane thrust is zero; it then drops off steadily to 0.00036 rad/s at the end of the perigee burn. Turn rate during the apogee burn is nearly constant at 0.000054 rad/s.

The second example is identical to the first except for having four short perigee burns, as opposed to one long burn, as is shown on Fig. 8. The perigee burns use from 67 to 68.7 deg of longitude and take from 17.9 to 16.1 min. The actual transfer orbit is very similar to the impulsive transfer orbit, with $e=0.723$ and $i=26.5$ deg. This transfer uses 62.37% of the initial spacecraft mass, for 10.67% greater payload than example 1. Total trip time is 14.3 h and gravity loss is 166 ft/s, down from example 1 by a factor of 10.

The behavior of the thrust direction is shown in Figs. 9 and 10. The in-plane thrust component shows less variation than in example 1. It does not always point inward of the velocity vector during the first three burns. The out-of-plane thrust is fairly constant; again, the bulk of the plane-change is during the apogee burn. The turn rate of the optimal thrust vector is relatively constant, in accord with the high-acceleration analysis. Variation is about 10% during each burn, with maximums of 0.00103 to 0.00098 rad/s at perigee and about 0.00004 rad/s at apogee.

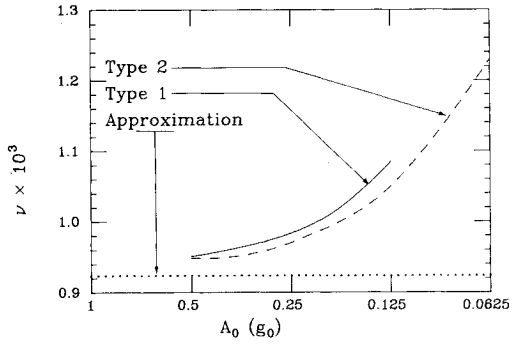

Fig. 11 ν vs initial acceleration.

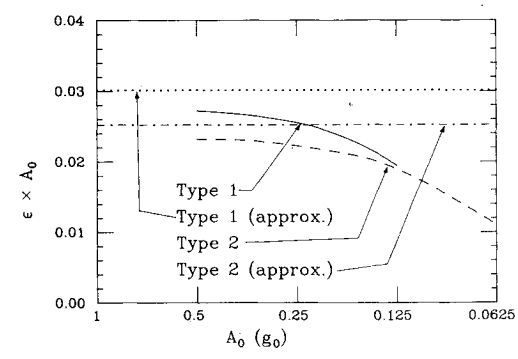

Fig. 12 ϵ vs initial acceleration.

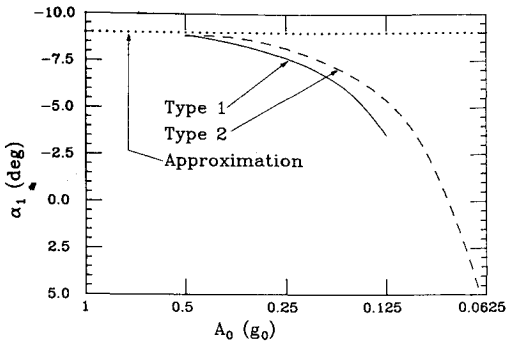

Fig. 13 α_f vs initial acceleration.

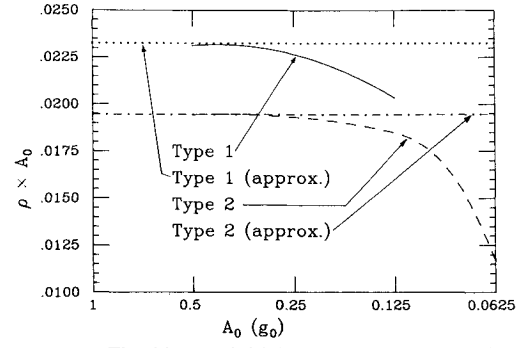

Fig. 14 ρ vs initial acceleration.

These fixed-thrust examples are representative of other types of transfers, such as fixed-acceleration. The behavior of the thrust vector is very similar. For given burn numbers, there is the same tendency for the transfer orbit to become larger, less eccentric, and less inclined as acceleration is lowered. Thrust vector turn rates become greater and less constant, as does the out-of-plane thrust. Thus the assumptions of the high-acceleration analyses are violated increasingly as the acceleration level drops and the gravity loss increases. It is therefore no surprise that the formulas of the preceding sections become inaccurate.

The change in the various initial adjoint parameters due to lowering initial acceleration is illustrated in Figs. 11-14 for both transfer types. The specific numbers are for single perigee burn transfers, but recalling the discussion of the previous sections, the figures give good estimates of the parameters for transfers with greater numbers of burns, by replacing A_0 with NA_0. Not shown is the behavior of $\Delta\theta_0$ and $\Delta\theta_f$. $\Delta\theta_0 \times A_0$ remains constant at the predicted value until $A_0 < \frac{1}{8}\, g_0$, when it begins to increase; $\Delta\theta_f \times A_0$ is constant to about the same point, when it starts to decrease.

Gravity loss vs acceleration and numbers of perigee burns for fixed-acceleration transfers is shown in Fig. 15 (similar behavior is observed for fixed-thrust). Robbins's formula suggests that L increases as $1/A_0^2$ and decreases roughly as $1/N^2$ [see Eq. (72)]; this is seen to be correct provided L is sufficiently small. Above 1000 ft/s or so, the approximate L is generally worse than the actual, and Robbins's formula gives increasingly perssimistic results. Note that as N increases and A_0 decreases, the gravity loss at apogee becomes a factor. Past this point it is preferable, i.e., transfers can have lower loss for the same time, if multiple apogee burns are performed while the number of perigee burns is somewhat reduced (see Ref. 1).

Further Notes

1) Coplanar transfers represent a simpler subcase of the full three-dimensional problem. Here, $\Delta\theta_0$ is undefined and ρ and α_f are zero, so that the problem reduces to trying to match r_f and v_f by varying ϵ and $\Delta\theta_f$.

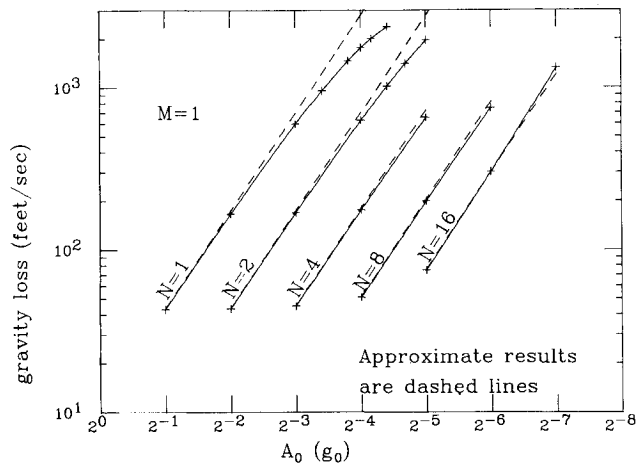

Fig. 15 Gravity loss vs acceleration and numbers of burns for fixed-acceleration transfers.

2) Our problem is formulated as the time-free problem, for which the Hamiltonian is zero in all cases. If the transfer time is constrained to be slightly below the value necessary for a particular time-free transfer, a higher-loss, nonzero Hamiltonian transfer can be computed using the same numbers of burns. However, as the time limit is lowered, the loss rises very rapidly to the loss for a much lower time, fewer-burn time-free transfer, which then is preferable. The range of time limits that lead to constrained-time solutions is a very small part of the total time range, so it will be possible to meet most mission requirements with a time-free transfer.

Extremely high-loss transfers are an exception: time free transfers do not exist in certain cases, perhaps forcing adoption of a constrained-time formulation (see Ref. 7).

3) A question arises: How much better is optimal thrust pointing than other, simpler control laws, such as horizontal thrust or tangential thrust? An analysis has been done for high-acceleration, coplanar LEO-GEO transfer using these two nonoptimal control laws. Comparing the results of this analysis with Robbins's formula, it is found that horizontal thrust increases gravity loss by 34% and tangential pointing by only 7.5%.

Conclusions

Optimal orbit transfer from a low circular orbit to a high circular orbit is discussed. Lawden's "primer vector" theory is preferred, as it allows exact, optimal solutions while giving detailed information on the spacecraft's thrust direction history. Impulsive and near-impulsive transfers are analyzed. Computer solution of low-thrust transfers is discussed. Results are presented for transfer to geosynchronous orbit. Robbins's formula for gravity loss is compared with exact results.

References

[1] Redding, D.C., "Highly Efficient, Very Low Thrust Transfer to Geosynchronous Orbit: Exact and Approximate Solutions," *Journal of Guidance, Control, and Dynamics,* Vol. 7, March-April 1984, pp. 140-147.

[2] Spencer, T.M., Glickman, R., and Bercaw, W., "Low Thrust Orbit Raising for Shuttle Payloads," *Journal of Guidance, Control and Dynamics,* Vol. 5, July-Aug. 1982, pp. 372-378.

[3] Edelbaum, T.M., Sackett, L.L., and Malchow, H.L., "Optimal Low Thrust Geocentric Transfer," AIAA Paper 73-1074, Lake Tahoe, Nevada, Oct. 31-Nov. 2, 1973.

[4] Lawden, D.F., *Optimal Trajectories for Space Navigation,* Butterworths, London, 1963.

[5] Danby, J.M.A., "The Matrizant of Keplerian Motion," *AIAA Journal,* Vol. 2, Jan. 1964, pp. 16-19.

[6] Robbins, H.M., "An Analytical Study of the Impulsive Approximation," *AIAA Journal,* Vol. 4, Aug. 1966, pp. 1417-1423.

[7] Redding, D.C., "Optimal Low Thrust Transfers to Geosynchronous Orbit," Ph.D. Thesis, Stanford University, Stanford, California, Oct. 1983.